20 NUMERICAL ANALYSIS OF COMBUSTION CHARACTERISTICS IN SI ENGINE WITH METHANOL REFOMULATED

Suk-Young Lee[1], Ku-Seob Jeong[2], Chung-Hwan Jeon[1], Young-June Chang[1]

[1] Department of Mechanical Engineering, Pusan National University 30 Jangjeon-dong, Geumjeong-gu, Busan 609-735, Korea

[2] Department of Automotive Engineering, jinju International University, 270 Sangmoonri, Moonsaneub, Jinju city, 609-735, korea

Abstract

This research is to estimate the possibility of using methanol reformulated fuel without modification of engine. The data obtained from the experiment are used for the numerical analysis. Methanol reformulated fuel has a higher burning speed, and heat release rate is proportional to burning speed. This is caused that the maximum heat release rate is larger and methanol reformulated fuel reaches the maximum sooner than the gasoline fuel. As engine speed increases under low-load condition, the difference in turbulent burning speed increases. On the contrary, the fuel characteristic difference decreases under high-load condition of 9.2kgf-m. The lowest turbulent burning speed is shown in unstable condition of 1500rpm and 9.2kgf-m. In the same condition, gasoline shows a larger decease than that of methanol reformulated fuel. Therefore, it is considered that methanol reformulated fuel is more suitable for operation because of better stability. Gas temperature in cylinder is higher for methanol-reformulated fuel because of higher burning speed and shorter quenching length. Therefore, it causes NO emission to increase but it produces less NO due to influence of chemical reaction dynamics and lower flame temperature respectively. Methanol reformulated fuel has higher CPL than that of gasoline fuel, and this is related to burning speed. As burning speed increases, the pressure increase rate also increases causing an abrupt combustion sound.

***Keywords* : Methanol reformulated fuel, Cycle by cycle variation, Break specific fuel consumption,Exhaust emissions, Noise and vibration**

Nomenclature

Alphabetics

A Area (m^2)
CPL Cylinder pressure level (dB)
C_p Specific heat in constant pressure (J/kg・K)
ff Turbulent flame coefficient
n Order number of noise
m mass (kg)
P Pressure (N/m^2)
Q Heating value (J)
R Universal gas constant (J/kg・K)
r Radius (m)
S Speed (m/s), frequency component
T Temperature (K)
t Time(sec)
U Internal energy (J)
u Turbulent intensity (m/s)
V Volume (m^3)
x Mass fraction burned

Greeks

γ Specific heat ratio
θ Crank angle (degree)
ρ Density (kg/m^3)

Subscript

c Cylinder
cr Crevice
b Burnt
ht Heat transfer
u Unburnt

Superscript

m, n Constant

1. Inroduction

Recently, the regulation of fuel itself has been getting stricter also. According to the World-Wide Fuel Charter, unleaded gasoline fuel has been classified into four different categories for fuel quality related to emission regulations (ACEA, 2000). They consist of Category 1-4 and detailed explanations are given in Appendix. The fuel for SI engines is mainly gasoline, which is a mixture of over 200 different hydrocarbons that consist of C4~C12 with low boiling points relative to the refine processes (ACEA, 2000). These are separated by 4 different components such as paraffin (C_nH_{2n+2}), olefin (C_nH_{2n}), naphthene (C_nH_{2n}) and aromatic series (C_nH_{2n-6}). Olefins are unsaturated hydrocarbons and, in many cases, are also good octane components of gasoline. However, olefins are thermally unstable and may lead to gum formation and deposits in an engine's intake system. Furthermore, their evaporation into the atmosphere as chemically reactive species contributes to ozone formation and their combustion products form toxins. So, it is restricted to below 20% volume fraction now and will be constrained to below 10% volume fraction . Aromatic components have such a high hydrocarbon density with an unsaturated ring structure as in double carbon-carbon bonds that they have a high energy content per unit volume, and have a high octane number. So they are used for important functions against knock, but cause troubles such as smoke generation and the dissolution of gasket materials due to high solvency characteristics and can increase engine deposits and tailpipe emissions, including CO_2. The fuel quality recommendation is restricted below 35% volume fraction or less. Especially in the case of benzene, it is well known for improving octane number, but is regulated below 2.5% volume fraction to avoid toxicity and will be reduced below 1% volume fraction

(Kwon et. al., 1999). Alas four (1997) studied the characteristics of performance, brake specific fuel consumption (bsfc) and thermal efficiency under the conditions of wide-range fuel/air equivalence ratios (Φ=0.8~1.3) for 30% volume alcohol (methanol and butanol)-gasoline blended fuels as well as pure gasoline in a single cylinder engine. Also Abdel-Rahman et al (1997) studied the effects of the compression ratio and blending volumes of up to 40% on SI engine performance. Moses et al (1995) studied the effects of methanol admixture on gasoline knocking in SI engine. Li et al (1995) investigated the effects of blended methanol on hydrocarbon oxidation and auto-ignition in a single cylinder S.I. engine. As mentioned above, the bulk of the research has studied not reformulated alcohol fuels but most blending fuels under constant speed and load conditions (Cho et. al., 2003 ; Yoon et. al., 2001). Recently, it came possible to predict combustion and gas flow in an engine by simulations. And the result of the prediction is used as a basis of research or an improvement of performance in an engine. As the prediction by simulation had merit to obtain a result of a research which is impossible to make a experiment, lots of simulation-related models were developed about combustion and gas flow. Therefore, in this search, methanol reformulated which was to substitute gasoline fuel without any alternation of hardware structure and electric control device of existing engine, gasoline and LPG fuel were compared through numerical analysis. Those like combustion, heat transfer model, chemical equilibrium combustion model, non equilibrium model and Fourier series model were established and Those like heat release rate, mass fraction burned, mean gas speed, burning speed, turbulent intensity, NO emission and noise was time-functionally calculated and compared with the experiments. These were all to analysis the combustion characteristics.

Table 1. Comparison of experimental fuel properties.

Item	Gasoline	RM 50
Fuel composition Vol. (%)	Gasoline 100%	Methanol 54% Aromatic 23% Non-aromatic 23%
Benzene content Vol. (%)	0.86	0.04
Olefin content Vol. (%)	17.5	0.30
Carbon fraction Wt. (%)	84.46	62.89
Hydrogen fraction Wt. (%)	13.89	12.59
Oxygen fractio Wt. (%)	1.65	24.53
Vapor pressure (kPa)	68.65	71.59
Specific gravity (15/4℃)	0.7228	0.7797
Octane number (RON)	92.2	121.0
LHV (kJ/kg)	41993	31024

Table 2. Specifications of experimental engine.

Item	Specification
Engine type	In-line 4 cylinder, SI engine
Valve mechanism	DOHC
Displacement (cc)	1799
Bore × Stroke (㎜)	81.6 × 86.0
Compression ratio	9.8

2. experimental setup

2.1 Fuel

Generally methanol has similar contents with aromatics in terms of high octane rating, and also has oxygenated functions (OH hydroxyl) to reduce exhaust emissions such as smoke. Even now most experiments using both methanol and gasoline fuel use blended gasoline with methanol for some volume fraction. But in this experiment, methanol-reformulated fuel that mixes methanol with the aromatics and non-aromatics of gasoline fuel is used. Table 1 gives the properties and characteristics of gasoline and reformulated fuels. We call these fuels gasoline and RM50 respectively. LHV(low heating value) of RM50 fuel has lower level due to the lower LHV of methanol. But RM50 has some advantages including higher octane number and oxygen fraction due to methanol.

2.2 Apparatus and Methods

Table 2 shows the specifications of the modern production engine used in this study. The schematic diagram of the experimental setup is shown in Figure 1. The engine is operated with a conventional ECU and the pressure sensor of the spark plug type measures the combustion pressure. Other signals such as the engine revolution, the injection timing and duration, the ignition timing, the oxygen sensor voltage, the wide band O_2 sensor signal, the intake air temperature and exhaust gas temperature are taken simultaneously by a data acquisition board.

For the measuring of the air/fuel ratio for experiment condition, the wide band oxygen sensor mounted at the exhaust pipe is used. And a stepping motor is installed to control the throttle valve-opening ratio at the throttle body. The experiment is carried out between the range of 231K to the cooling water temperature and of 241K to the intake air temperature. In this experiment, the conventional ECU is used and the accelerating range is from 1500 rpm to 2500 rpm since this range is applicable to typical the driving range. The load are 4.6 and 9.2kgf-m, which are a quarter and a half of a full load of this engine. The engine-out exhaust gas in terms of NO is analyzed by exhaust emission analysis(Clean air I/M 2000), which is able to detect data per second. The calibration is conducted with standard gases.

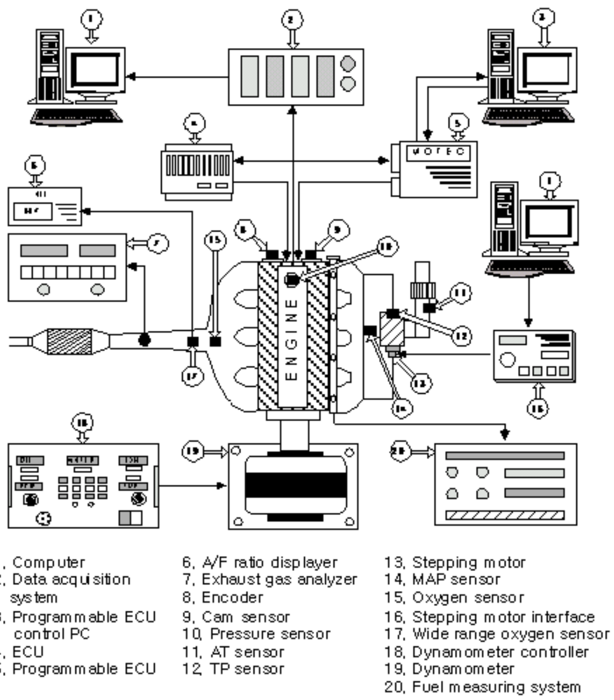

Figure 1. Schematic diagram of experimental apparatus

3.Numerical model

To analyze thermodynamic phenomenon in cylinder, the assumption about working fluid and exhaust emission is as follows,

1) Working fluid in cylinder is ideal gas and maintains thermodynamic equilibrium state.
2) Mixture in cylinder is homogeneous and doesn't react mutually.
3) Pressure in cylinder is constant wherever it may be.
4) Unburnt gas doesn't react chemically. 5) Exhaust emission is assumed to be chemical equilibrium.

3.1 One-zone model

3.1.1 Heat release rate

In figure 2, the formula which is to calculate the heat capacity in combustion is induced as following by the first law of thermodynamics in open system (Heywood, 1988).
Assuming working fluid is here ideal gas, as the equation of ideal gas is applied, it becomes as follows.

$$\frac{dQ}{d\theta} - P_c\frac{dV_c}{d\theta} = \frac{dU_u}{d\theta} + \frac{dQ_{ht}}{d\theta} + h_{cr}\cdot\frac{dm_{cr}}{d\theta} \quad (1)$$

$$\frac{dQ}{d\theta} = \frac{\gamma}{\gamma-1}P_c\frac{dV_c}{d\theta} + \frac{1}{\gamma-1}V_c\frac{dP_c}{d\theta} + \frac{dQ_{ht}}{d\theta} + h_{cr}\cdot\frac{dm_{cr}}{d\theta} \quad (2)$$

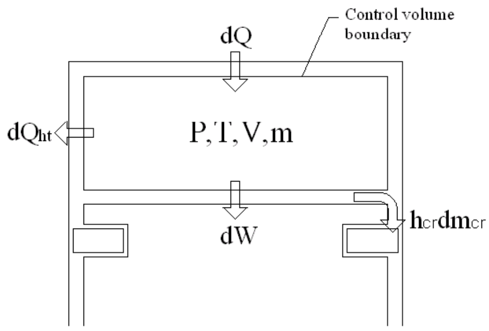

Figure 2. Combustion chamber model of engine

Table 3. Specific heat ratio for gasoline

x_b / ∅	Combustion process 3%	18%	33%	Expansion process
0.4	1.312			1.343-3.653×10$^{-5}T_c$
0.7	1.290			1.290-1.200×10$^{-5}T_c$
0.9	1.282	1.280	1.280	1.289-1.523×10$^{-5}T_c$
1.0	1.280	1.275	1.275	1.282-1.349×10$^{-5}T_c$
1.1	1.283	1.283	1.283	1.302-2.213×10$^{-5}T_c$
1.2	1.291	1.293	1.298	1.299-1.885×10$^{-5}T_c$

Table 4. Specific heat ratio for methanol

x_b / ∅	Combustion process 8.5%	22%	37%	Expansion process
0.7	1.258	1.253	1.240	1.314-2.937×10$^{-5}T_c$
0.9	1.265	1.270	1.271	1.391-7.829×10$^{-5}T_c$
1.0	1.260	1.271	1.282	1.449-1.162×10$^{-5}T_c$
1.1	1.239	1.242	1.245	1.331-4.454×10$^{-5}T_c$
1.2	1.214	1.215	1.215	1.287-1.962×10$^{-5}T_c$
1.3	1.192	1.192	1.191	1.276-1.185×10$^{-5}T_c$

3.1.2 Specific heat ratio

In combustion process, the specific heat ratio was used the combustion characteristic instead of the property of matter. So, in combustion and expansion process, the value which is presented by Chun and Heywood (1987) in table 3, and Cheung and Heywood (1993) in table 4 was used. The reformulated fuel was used after revision of data in tables 3 and 4 following component ratio.

3.2 Two-zone model

After the ignition happens in mixture, the gas in cylinder is divided into 2 zone of burnt and unburnt gas by flame area, and calculates as the 2 zone model. Inputting heat release rate to calculate above and the difference of temperature are calculated by using the first law of thermodynamics and ideal gas equation as follows (Bense et. al., 1975).

$$\frac{dT_u}{d\theta} = \frac{V_u}{m_uC_{pu}}\frac{dP_c}{d\theta} + \frac{1}{m_uC_{pu}}\frac{dQ_u}{d\theta} \quad (3)$$

$$\frac{dT_b}{d\theta} = \frac{P_c}{m_bR_b}\left[\frac{dV}{d\theta} - \left(\frac{R_bT_b}{P_c} - \frac{R_uT_u}{P_c}\right)\frac{dm_b}{d\theta} - \frac{R_uV_u}{P_cC_{pu}} - \frac{R_u}{P_cC_{pu}}\frac{dQ_u}{d\theta} + \frac{V_c}{P_c}\frac{dP_c}{d\theta}\right] \quad (4)$$

3.3 Flame and combustion

Laminar burning speed is calculated by the 2 zone temperatures to calculate above and the pressure in cylinder to measure by experiment as follows (Kuehl, 1962).

$$S_l = \left[\frac{1.087\times10^6}{\left(10^4/T_b + 900/T_u\right)^{4.938}}\right]P^{-0.09876} \quad (5)$$

Therefore, the volume of burnt gas is in equation(6) and flame radius, r_f , is calculated like equations(7) by trial and error method. Flame is assumed to spread in sphere shape, the expression is in equation(7).

$$V_b = V_c - V_u \quad (6)$$

$$V_b = \pi\int_0^{r_f\cos\theta} r_f^2\sin^2\frac{\theta}{2}dy + \pi\int_{r_f\cos\theta}^{r_f}\left(r_f^2 - y^2\right)dy \quad (7)$$

As the volume of burnt zone is a function of flame radius, and assuming flame spreads in sphere shape, it shows like equation(8).

$$A_f = 2\pi\int_{r\cos\theta}^{r}\sqrt{r^2-y^2}\,dy \quad (8)$$

The turbulent burning speed is calculated by the density of unburnt gas and the volume of burnt zone which is calculated in equation

$$S_t = \frac{dm_b/dt}{\rho_uA_f} \quad (9)$$

Starting combustion process in 4 segments, the coefficient of turbulent interpolation is calculated through assumption of different relational equation in each segment. The first segment is the period of ignition delay, the second segment is the period of flame growth from ignition to the point which flame radius is 0.03m. And the third segment is set until mass fraction burned reaches 50%, the forth is segment where burning speed diminishes. The equation about the first and second segment is as follows.

$$ff_{1,2} = \left(\frac{r_f}{0.03}\right)^{0.6}ff_3 \quad (10)$$

The flame coefficient of the third segment is derived from the experiment by Mattavi (1982) as follows.

$$ff_3 = 1 + 4.01\frac{u'}{u_l} \tag{11}$$

The forth segment, where flame speed diminishes, flame coefficient is expressed as following by relational equation that laminar and turbulent flame speed is equal in crank angle which combustion is finished.

$$ff_4 = ff_3\left[4\left(\frac{1}{ff_3} - 1\right)(x - 0.5)^2 + 1\right] \tag{12}$$

The turbulent intensity is calculated by equation (10), (11) and (12).

3.4 Emission

In a gasoline engine, CO_2, O_2, H_2O, and N_2, compromise the majority of the exhaust, followed by NO and soot, depending on the pressure and temperature. CO is generally not a major component of diesel exhaust. The gas components CO_2, O_2, H_2O, and N_2, have a relatively short reaction time as compared to the combustion time, and were calculated using equilibrium equations. NO, however, takes a long time to reach equilibrium and was calculated using non-equilibrium equations.

The Zeldovich mechanism, the process of converting atmospheric nitrogen into NO, was used for the NO calculations in the combustion model. This mechanism is the most appropriate mechanism to apply to standard fuel-air mixtures in the combustion chamber. Moreover, the degree of fuel-air mix-ratio differs depending on the location in the combustion chamber. Some researchers divide the combustion chamber into multiple zones in order to calculate emissions in the separate zones, and then average the results. In the current research, however, the exhaust was calculated under a model that assumes a homogeneous mixture in the combustion chamber, and that the chamber has one zone.

3.5 Noise

To investigate the frequency component in contrast to pressure in cylinder, which is obtained in experiment, the pressure is expanded by Fourier's series as following.

$$P(\theta) = \frac{1}{2}a_0 + \sum_n (a_n \cos\frac{n}{2}\theta + b_n \sin\frac{n}{2}\theta) \tag{13}$$

In equation (13), as it takes a 4 cycle engine as a subject, a half of engine rotation is set on the basis of the order. While is defined as each frequency component, it is expressed as follows.

$$S_n = \sqrt{a_n^2 + b_n^2} \tag{14}$$

A CPL is defined as the value to calculate frequency component, to sound pressure level, it is expressed as follows.

$$(CPL)_n = 20\log_{10}(S_n / 2.8861) + 200 \quad (dB) \tag{15}$$

4. RESULTS AND DISCUSSIONS

In this chapter, the experimental results of exhaust emission and noise are compared with the results of numerical analysis, and combustion and noise characteristics of each fuel are analyzed.

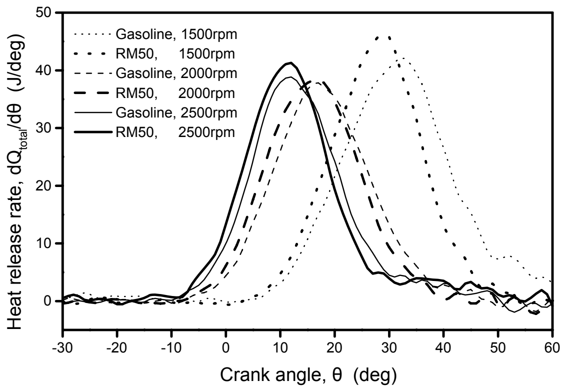

Figure 3. Comparison of heat release rate versus crank angle for each fuel at 9.2 kgf-m load

4.1 Heat Release Rate

Comparison of heat release rate of each fuel is shown in figure 3. Generally, heat release rate increases as the load increases and engine speed decreases, because duration per crank angle in a cycle decreases along with an increment of engine speed. The curve of RM50 shows more ahead than that of gasoline because RM50 has a faster burning speed. The maximum heat release rate is proportional to burning speed, and it reaches the maximum quicker as burning speed increases. In the condition of 1500rpm and 9.8kgf-m, it shows an unstable operating condition caused by excessive load compared to engine speed. The heat release rate curve shows that RM50 is more stable than gasoline, because of wider combustion limitation range. And, in this case, the maximum heat release rate increase, consequently, a large amount of fuel is burnt to generate a higher torque under an unstable condition.

4.2 Turbulent Burning Speed and Intensity

Turbulent burning speed according to crank angle is shown in Figure 4. Generally, in the low-load condition of 4.6kgf-m, fuel characteristics are well showed and the maximum turbulent burning speed is greater than that of 9.8kgf-m high-load condition.

Also the difference between average turbulent burning speeds of each fuel is greater in low-load condition as shown in Fig. 4, however difference caused by fuel characteristics is merely seen under the condition of 1500rpm and 4.6kgf-m. Fig. 4 also shows that difference in turbulent burning speed for each fuel increases as engine speed increase under low-load condition. On the contrary, fuel characteristics are diminished under the high-load condition of 9.2kgf-m and the maximum turbulent burning speed is lower than that of 4.6kgf-m low-load condition. Moreover, the difference between average turbulent burning speeds is less than. The lowest average turbulent burning speed is showed in the unstable condition of 1500rpm and 9.2kgf-m and gasoline has been reduced more. Therefore, RM50 seems to contribute a larger portion for operation stability than gasoline. The average turbulent burning speeds of gasoline and RM50 are compared for difference load conditions of 9.2kgf-m and 4.6kgf-m. As the results, 3.0, 1.0, 1.4m/s reductions are recorded for gasoline, and 2.6, 1.6, 3.0m/s reductions are recorded for RM50 under the conditions of 1500, 2000, 2500rpm respectively. These results represent a reduction in turbulent burning speed of both RM50 and gasoline when load increases. Figure5, 6 shows the turbulent intensity. Generally, it tends to be very similar with the curve of turbulent burning speed, and difference in the maximum values of RM50 and gasoline gets larger as engine speed increases.

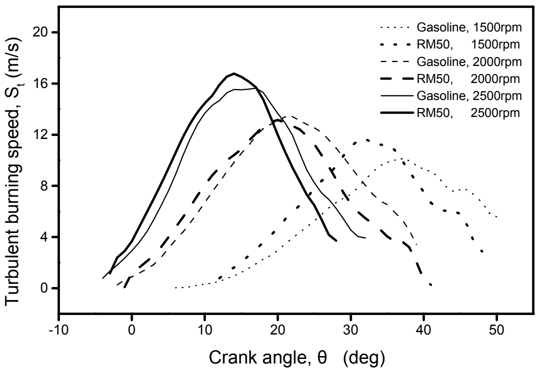

Figure 4. Comparison of turbulent burning speed in cylinder versus crank angle for each fuel at 9.2 kgf-m load

The average turbulence intensity is showed in Figure 7. In this figure, turbulence intensity tends to increase as engine speed and load increase, and fuel characteristics are clearly shown in the low-load condition. In the unstable condition of 1500rpm and 9.2kgf-m, the turbulent intensity reduces the greatest amount, but RM50 shows 0.08m/s higher than gasoline. Therefore, RM50 is more efficient for combustion in the unstable condition.

4.3 NO emission

Time taken for NO concentration to reach an equilibrium is usually longer than any other emissions. Therefore, the calculation of NO emission is divided into two steps, which are thermodynamic equilibrium and non-equilibrium.

In the combustion process, NO reaches an equilibrium concentration quicker because of a faster reaction speed due to high gas temperature in cylinder, and NO concentration increases without freezing as shown in fig. 8. However, in the expansion process, NO takes a long time to reach an equilibrium and freezes because it slows down to react due to a lower temperature. The freezing is known as status occurred by speed of reaction and inverse reaction being equalled in dissociation of O_2, N_2 and NO (Newhall et. al., 1967). In Figure 8, the freezing keeps it stable, even temperature and pressure drop in the expansion process. Also RM50 has a higher burning speed and a shorter quenching length, causing a high gas temperature in cylinder. Therefore, it causes an increment of NO emissions, however, on the other hand, it produces less NO emissions due to chemical reaction dynamics and lower flame temperature respectively. In the part load condition, it takes a long time to reach an equilibrium because in-cylinder temperature is lower

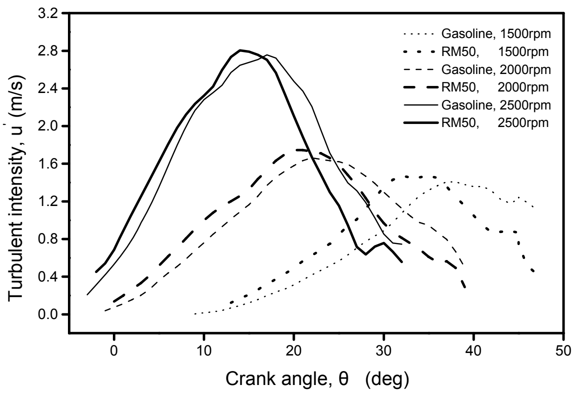

Figure 5. Comparison of turbulent intensity in cylinder versus crank angle for each fuel at 9.2 kgf-m load

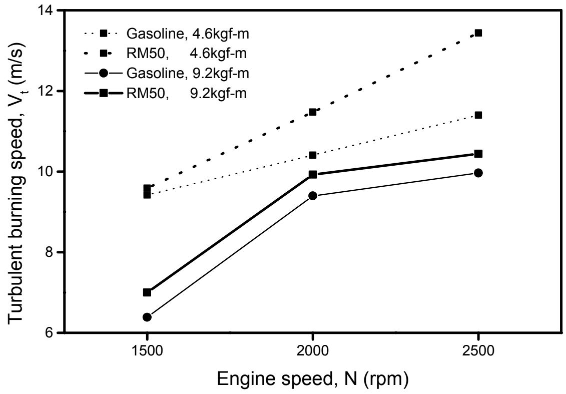

Figure 6. Comparison of mean turbulent burning speed in cylinder versus engine speed for each fuel at each condition

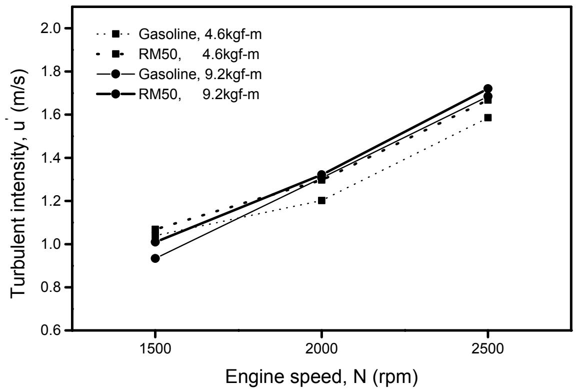

Figure 7. Comparison of mean turbulent intensity in cylinder versus engine speed for each fuel at each condition

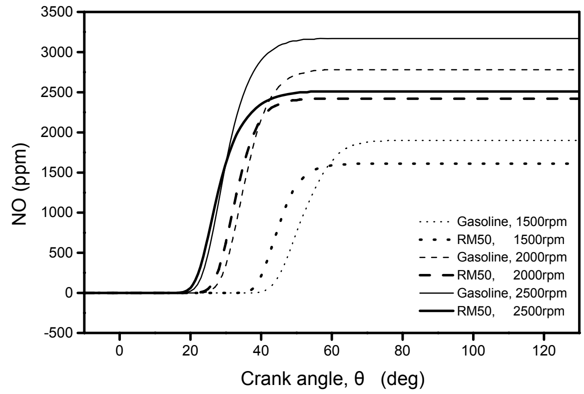

Figure 8. Comparison of NO calculated at 9.2 kgf-m load

and reaction speed is more slow. Therefore, the constant value can be observed from the point of the maximum NO concentration as freezing condition. Also difference in NO emissions increases as load increase in the part load condition. Therefore, when NO emission is predicted by using RM50, in-cylinder temperature of low heating value and combustion characteristics including burning speed need to be considered.

4.4 Noise

Figure 9 is the calculated result of CPL according to frequency for each fuel under part load condition. Generally, CPL for RM50 is higher than gasoline because of an increase in pressure

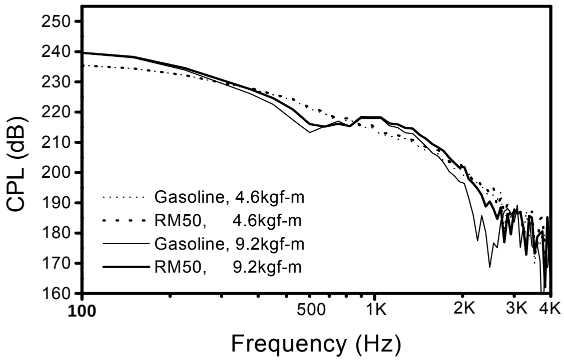

Figure 9. Comparison of CPL for each fuel at 1500RPM

increase rate caused by a faster burning speed. Also the difference decreases as engine speed increases, because fuel characteristics decrease as engine speed increase as it is mentioned above. Especially, it tends to reduce at 1kHz approximately in high load condition, and increase again afterward.

5 Conclusion

This research is to estimate the possibility of using RM50 without modification of engine. The data obtained from the experiment are usedfor the numerical analysis. The analysis of combustion and noise characteristics of methanol reformulated fuel is as follows.

(1) Because RM50 has a higher burning speed, the maximum heat release rate is larger and RM50 reaches the maximum sooner than the gasoline fuel. Heat release rate is proportional to burning speed.

(2) RM50 has shorter combustion duration than the gasoline, and this is caused by a wider combustion limitation range. Furthermore, differences of combustion duration and ignition timing between each fuel tend to decrease as engine speed increases.

(3) As engine speed increases under low-load condition, the difference in turbulent burning speed increases. On the contrary, the fuel characteristic difference decreases under high-load condition of 9.2kgf-m. The lowest turbulent burning speed is shown in unstable condition of 1500rpm and 9.2kgf-m. In the same condition, gasoline shows a larger decease than that of RM50. Therefore, it is considered that RM50 is more suitable for operation because of better stability.

(4) The difference of turbulent intensity increases as engine speed and load increase, and fuel characteristics are well shown especially under low-load condition.

(5) Gas temperature in cylinder is higher for RM50 because of higher burning speed and shorter quenching length. Therefore, it causes NO emission to increase but it produces less NO due to influence of chemical reaction dynamics and lower flame temperature respectively. Consequently, combustion characteristics need to be considered, in addition to temperature in cylinder by low heating value, to estimate NO emission when RM50 is used.

(6) RM50 has higher CPL than that of gasoline fuel, and this is related to burning speed. As burning speed increases, the pressure increase rate also increases causing a abrupt combustion sound. A decrease of noise in difference can be observed when engine speed increases and this is a result of a decrement of effect by fuel characteristics according to an increment of engine speed.

Refferences

[1] Abdel-Rahman, A. and Osman, M., 1997, "Experimental Investigation on Varying the Compression Ratio of SI Engine Working under Different Ethanol-Gasoline Fuel Blends," Int. J. Energy Research, Vol. 21, pp. 31-40.

[2] ACEA, Alliance, EMA, JAMA, 2000, World-Wide Fuel Charter. pp. 1~51.

[3] Alasfour, F, 1997, "A Single Cylinder Engine Study : Engine Performance," Int. J. Energy Research, Vol. 21, pp. 21~30.

[4] Cho, H. and Lee, C., 2003, "A Study on Combustion and Emission Characteristics of Methanol Blended Fuel in SI Engine," Transactions of KSAE, Vol. 11, No. 6, pp. 1~6.

[5] Korotney, D., Rao, V., Lindhjen, C. and Sklar, M., 1995, "Reformulated Gasoline Effects on Exhuast Emissions: Phase Ⅲ: Investigation on the Effects of Sulfur, Olefins, Volatility, and Aromatics and the Interactions Between Olefins and Volatility or Sulfur," SAE Paper No. 950782.

[6] Kwon, Y., Bazzani, R., Bennett, P., Esmilaire, O., Scorletti, P., Morgan, T., Goodfellow. C,, Lien, M., Broeckx, W. and Liiva, P., 1999, "Emissions Response of a European Specification Direct-Injection Gasoline Vehicle to a Fuels Matrix Incorporating Independent Variations in Both Compositional and Distillation Parameters," SAE Paper No. 1999-01-3663.

[7] Li, H., Prabhu, S., Miller, D. and Cernansky, N., 1995, "The Effects of Methanol and Ethanol on the Oxidation of a Primary Reference Fuel Blend in an Motored Engine," SAE Paper No. 950682.

[8] Moses, E., Yarin, A. and Bar-Yoseph, P., 1995, "On Knocking Prediction in Spark Ignition Engines," Combustion and Flame, Vol. 101, pp. 239~261.

[9] Heywood, J. B., 1988, "Internal Combustion Engine Fundamentals. Mc-Graw-Hill," New Tork. pp. 383~390, 413~423.

[10] Newhall, H. K. and Starkman, E. S., 1967, "Direct Spectroscpics Determination of Nitric Oxide in Reciprocating Engine Cylinders," SAE Paper No. 670122.

[11] Chun, K. M. and Heywood, J. B., 1987, "Estimating Heat Release and Mass of Mixture Burned from SI Engine Pressure Data," Combust. Sci and Tech. Vol. 54. pp. 133-143.

[12] Cheung, H. M. and Heywood, J. B., 1993, "Evaluation of One-Zone Burn Rate Analysis Procedure using Production SI Engine Pressure Data," SAE Paper No. 932749.

[13] Bense, R. S., Annand, W. J. D. and Baruah, P. C., 1975, "A Simulation Model including Intake and Exhaust System for a Single Cylinder 4-stroke cycle SI Engine," Int. J. Mech. Sci. Vol. 17(2). pp. 97~124.

[14] Kuehl, D. K., 1962, "Laminar Burning Velocity of Propane-Air Mixture. 8th International Symposium on Combustion," pp. 510~521.

[15] Mattavi, J. N., 1982, "Effects of Combustion Chamber Design on Combustion in Spark ignition Engines," SAE Paper No. 821578.